

Research Article

Gas-Supported High-Photoactivity TiO₂ Nanotubes

Sheng Wang, Tao Wang, Yuanwei Ding, Youfeng Xu, Qiying Su, Yanlong Gao, Guohua Jiang, and Wenxing Chen

Key Laboratory of Advanced Textile Materials and Manufacturing Technology of Ministry of Education, Zhejiang Sci-Tech University, Hangzhou 310018, China

Correspondence should be addressed to Sheng Wang, wangsheng571@hotmail.com

Received 18 October 2012; Accepted 28 November 2012

Academic Editor: Xijin Xu

Copyright © 2012 Sheng Wang et al. This is an open access article distributed under the Creative Commons Attribution License, which permits unrestricted use, distribution, and reproduction in any medium, provided the original work is properly cited.

By changing hydrothermal condition and post-heat-treatment temperature, silica-coated TiO₂ nanotubes are obtained successfully. The effects of gas-supported process on tubular morphology, crystallinity, and photocatalytic activity are discussed. It is found that the sample prepared at hydrothermal treatment (180°C/9 h) and calcination (650°C/2 h) shows perfect open-ended tubular morphology and increased crystallinity. The photoactivity of the sample is proved to be 5 times higher than that of TiO₂ nanoparticles.

1. Introduction

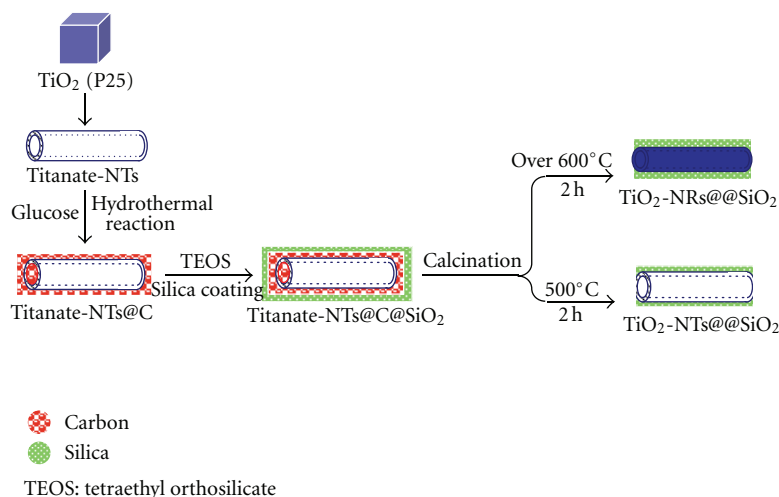
TiO₂-based nanomaterials have been intensely investigated due to its applications in air purification, water disinfection, hazardous water remediation, and other fields since Honda and Fujishima discovered the photocatalytic splitting of water on the TiO₂ electrodes in 1972 [1–5]. In particular, TiO₂ nanotubes (TiO₂-NTs) with high surface area, porosity, low cost, and chemical stability are attracting considerable attention, as compared with other nanostructures, and would be good candidates for potential applications in photocatalysis, gas sensing, pigments, photovoltaic applications, solar cells, and water detoxification applications [6–10].

On the other hand, as we know, photocatalytic activity is a comprehensive parameter, which is affected by many factors such as morphology, crystallinity, surface area, doping elements, and so on. However, it is very difficult to adjust each factor alone during the preparation process of nanomaterials. For instance, high-quality hydrogen titanate nanotubes (Titanate-NTs) can be obtained by a simple hydrothermal treatment of crystalline TiO₂ particles with NaOH aqueous solutions. But the as-prepared products are predominately in amorphous phase, shows low photocatalytic activity. Therefore, since their photocatalytic performance is closely related to crystallinity, additional

crystallization is always required for those products. Unfortunately, such materials are also prone to collapse during the calcination process. As a result, the tubular morphology is destroyed, with a significant decrease in specific surface area (S_{BET}), pore volume, and photocatalytic activity [11–13].

How to adjust both morphology and crystallinity to improve photocatalytic activity of TiO₂-NTs is a challenging subject for us. In our previous work, we presented a simple chemical morphology-freezing method, at post-heat-treatment process by combustion of filled carbon in titanate nanotubes to obtain gas-phase support of CO₂, and after calcination at 500°C we obtained high photoactivity TiO₂/SiO₂ nanotubes (TiO₂-NT_S@SiO₂) with perfect one-dimensional tubular morphology and fine crystal form for photocatalysis, which is 4 times higher than TiO₂ nanoparticles (P-25) [14].

In this work, we find, during the gas-supported process, that phase transfer temperature of TiO₂ from anatase to rutile is delayed by combustion of carbon to CO₂. By using this phenomenon, we improve the preparation method and obtain TiO₂ nanotubes with perfect open-ended tubular morphology and increased crystallinity at much higher temperature. The photoactivity of sample is proved 5 times higher than TiO₂ nanoparticles.



SCHEME 1: Formation process of $\text{TiO}_2\text{-NTs}@@\text{SiO}_2$ (500°C , 2 h) and $\text{TiO}_2\text{-NRs}@@\text{SiO}_2$ (Over 600°C , 2 h).

2. Experimental Details

2.1. Synthesis of $\text{TiO}_2\text{-NTs}@@\text{SiO}_2$ Tubular Nanocomposites. $\text{TiO}_2\text{-NTs}@@\text{SiO}_2$ nanocomposites were prepared by using chemical morphology freezing method that was described in our previous work [14]. First, hydrogen titanate nanotubes (Titanate-NTs) were prepared, and a carbon layer was coated on Titanate-NTs by hydrothermal treatment to prepare carbon-coated Titanate-NTs (Titanate-NTs@C). Then a second silica layer was followed to coat onto Titanate-NTs@C via a conventional alkoxide sol-gel method (Titanate-NTs@C@ SiO_2). Finally the sample was calcined and the carbon layer was combusted to yield $\text{TiO}_2\text{-NTs}@@\text{SiO}_2$ tubular nanocomposites.

2.2. Characterization. Transmission electron microscopy (TEM) samples were prepared by suspending the nanoparticles in ethanol and then casting on a holey, carbon-coated Cu grid. High-resolution TEM images were obtained with a JEM-2010(HR) instrument operating at 200 kV. Energy dispersive X-ray analysis (EDS, Inca Energy-200) was used to investigate the sample compositions. X Ray diffraction (XRD) patterns were obtained on a D/MAX-RB X-ray diffractometer (D/Max-2550pc), using $\text{Cu-K}\alpha$ radiation at a scan rate (2θ) of $0.05^\circ \text{ s}^{-1}$, and were used to determine the phase structure of the obtained samples. The accelerating voltage and the applied current were 15 kV and 20 mA, respectively. Specific surface area (S_{BET}) was determined using a Micromeritics Tristar 3000.

2.3. Measurement of Photocatalytic Activity. The photocatalytic activity of $\text{TiO}_2\text{-NTs}@@\text{SiO}_2$ was defined as the amount of CO_2 that resulted from the photocatalytic decomposition of methanol/water solution (5%, volume ratio). 40 mg sample was suspended in a solution of methanol (4 mL). The methanol vapor was allowed to reach adsorption-desorption equilibrium with catalysts in the reactor prior to UV light irradiation. Then the suspension was irradiated with UV light (500 W) at 25°C . After irradiation,

the generated CO_2 gas was collected with a syringe and analyzed by gas chromatography (6890N, Agilent) [13, 14].

3. Result and Discussion

3.1. CO_2 Gas-Supported $\text{TiO}_2\text{-NTs}@@\text{SiO}_2$. Open-ended Titanate-NTs, which with diameters of 4 to 7 nm and lengths of several hundred nanometers, were obtained by a hydrothermal reaction using Degussa P25 and 10 M NaOH aqueous solution at 150°C for 48 h (Scheme 1, Figure 1(a)). In order to obtain high photoactivity TiO_2 nanotubes, with perfect open-ended tubular morphology and fine anatase phase, Titanate-NTs were filled with LaMer-model carbon and then coated with a silica layer. This filling and coating process “isolates” microthermal deformation from the system and consequently prevents the destruction of the tubular morphology during the calcination process. After calcination at 500°C for 2 hours, $\text{TiO}_2\text{-NTs}@@\text{SiO}_2$ were obtained by CO_2 gas supporting and showed the higher photoactivity of all the samples, which is 4 times higher than TiO_2 nanoparticles (Figure 1(b)) [14].

On the other hand, it is generally accepted that crystallization is always an aggregation process from amorphous state, and crystals grow by attachment of ions to inorganic surfaces or organic templates [15]. Numerous researches describe the similar crystallization process of TiO_2 crystallites. With increasing calcination temperature from 400°C to 600°C , the crystallization of anatase phase improves, indicating that at high temperature amorphous Ti atoms move into anatase crystal location. Usually, the anatase phase starts to transform to rutile phase when the calcination temperature exceeds 600°C . Since anatase phase of TiO_2 is beneficial to photoactivity, it is believed that the phase transform temperature is the most optimal temperature to achieve perfect anatase phase of TiO_2 and best photoactivity as well.

However, in the CO_2 gas-supported process, it is observed that $\text{TiO}_2\text{-NTs}@@\text{SiO}_2$ nanocomposites keep as pure anatase phase even at 700°C , which indicates that phase

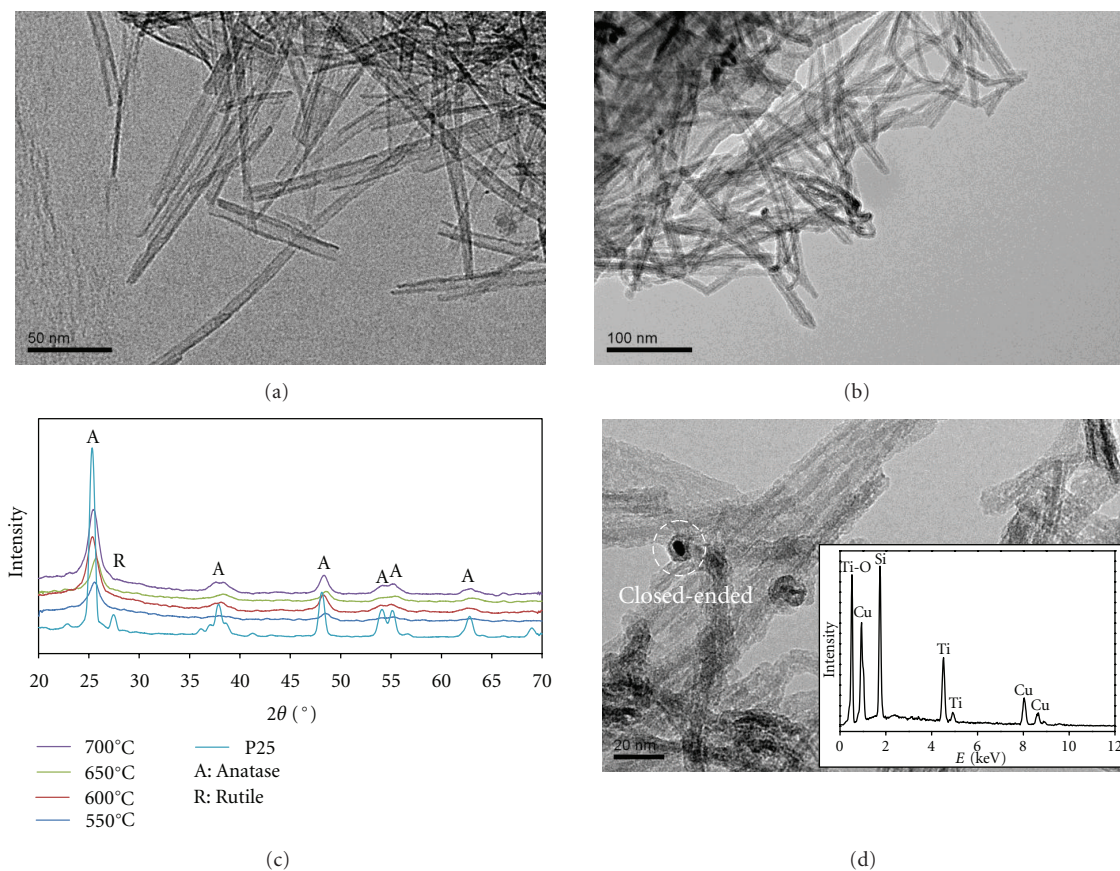


FIGURE 1: TEM images of (a) titanate nanotubes, (b) $\text{TiO}_2\text{-NTs@SiO}_2$ with “open-ended” structure (500°C , 2 h). (c) XRD pattern of $\text{TiO}_2\text{-NTs@SiO}_2$ calcined at various temperatures. (d) $\text{TiO}_2\text{-NRs@SiO}_2$ with “close-ended” structure (over 600°C , 2 h) and EDS spectra of the sample (inset).

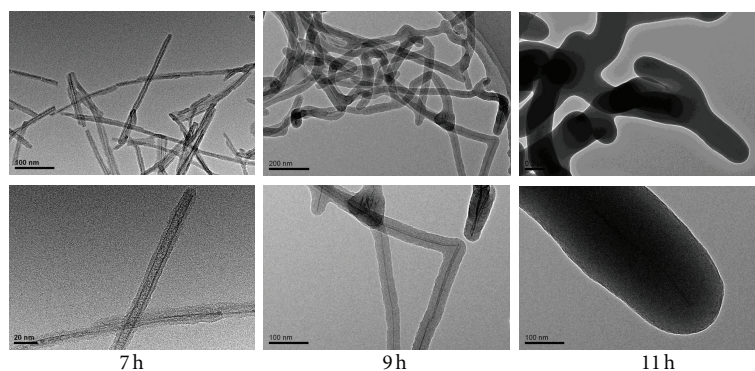


FIGURE 2: TEM images of Titanate-NTs@C under different carbon-treated hydrothermal reaction condition.

transfer temperature is delayed (Figure 1(c)). It is well known that the delay of phase transfer temperature is common in calcination process of nanoparticles doped with different elements, because doping with different types of elements will undoubtedly prevent migration of atom of host materials to the crystal location. However, it should be noted that EDS spectra of $\text{TiO}_2\text{-NTs@SiO}_2$ show that after the calcination,

evidence of Ti, Si, and O is found in sample and no carbon peak is observed, indicating the complete combustion of carbon in calcination process (Figure 1(d)). Moreover, XRD pattern of $\text{TiO}_2\text{-NTs@SiO}_2$ exhibits that no characteristic peaks of C are observed, indicating that C element has not been doped in crystal lattice of TiO_2 (Figure 1(c)). Therefore, the experiment results suggest that in gas-supported process,

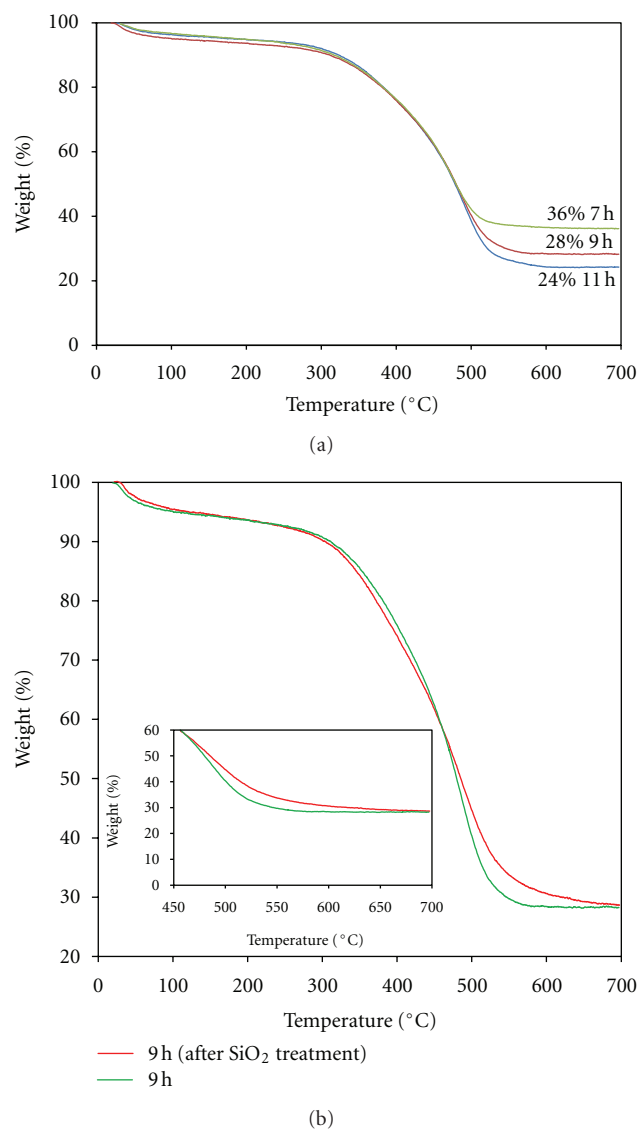


FIGURE 3: TG curves of (a) Titanate-NTs@C under different hydrothermal reaction time and (b) Titanate-NTs@C and Titanate-NTs@C@SiO₂ at 9 h hydrothermal reaction time.

the microcosmic migration of Ti atoms to the crystal location is prevented by CO₂ evolution, leading to the macroscopical delay of phase transfer temperature finally.

From our previous work, even after calcination at 500°C for 2 hours, some hydrogen titanate nanotubes may still have not been crystallized completely. If the remaining amorphous phase hydrogen titanate can be transformed into anatase phase completely, this will undoubtedly enhance the photoactivity of TiO₂-NTs. However, when the calcination temperature is increased to 600°C, the tubular morphology is significantly destroyed. As shown in Figure 1(d), only “close-ended” structure is observed, indicating that TiO₂-NTs has been collapsed and fused to TiO₂ nanorods (TiO₂-NRs@SiO₂). As mentioned above, photoactivity is a comprehensive factor that is related to temperature, crystallinity, specific surface area, and so on, so it is a challenge to obtain

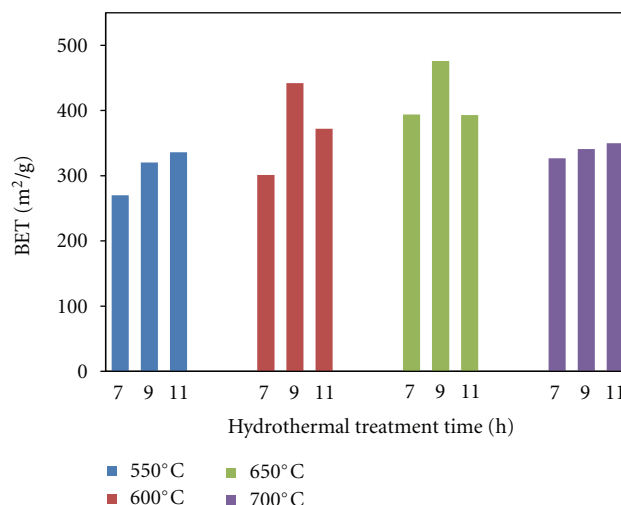


FIGURE 4: Specific surface area (S_{BET}) of Titanate-NTs@C@SiO₂ under different hydrothermal reaction condition and calcination temperature.

TiO₂-NTs with perfect tubular morphology at much higher temperature.

3.2. Improved Carbon-Treated Titanate Nanotubes. In order to keep the tubular morphology and large surface areas simultaneously at much higher calcination temperature, our strategy is to extend combustion time of carbon to support nanotubular morphology in gas-supported process. There are two options to select: one is to increase thickness of the silica coated layer to cut off air and retard combustion. However, experiment results showed such treatment always bring aggregation problem of silica itself and disadvantages in photocatalytic activity due to the excessively thick coating, which impeded mass transfer channel.

Therefore, it is a reasonable strategy to extend the combustion time by increasing the amount of carbon. The effects of the amount of carbon on the morphology and crystal structure of the nanotubes are studied at 180°C by changing the reaction time of carbon-treated hydrothermal reaction. As shown in Figure 2, after being carbon-treated for 7 h, titanate nanotubes with a diameter of 4 to 7 nm are covered with a carbon layer uniformly, and the thickness of carbon layer is about 3 nm. Extending the time of hydrothermal reaction, the thickness of carbon layer is increased effectively. The thickness of carbon layer is increased to about 20 nm for 9 h and over 120 nm for 11 h, respectively.

3.3. Thermogravimetric Analysis. The TG curves of the samples obtained at different hydrothermal reaction time (7 h, 9 h, 11 h) are shown in Figure 3(a). The curves are similar apparently except that each curve has a large weight loss at high temperature stage, which is considered as the combustion of carbon. It is observed that with increasing hydrothermal reaction time, weight loss of sample gradually increases, suggesting that the thickness and density of carbon layer increases linearly with the increase of hydrothermal

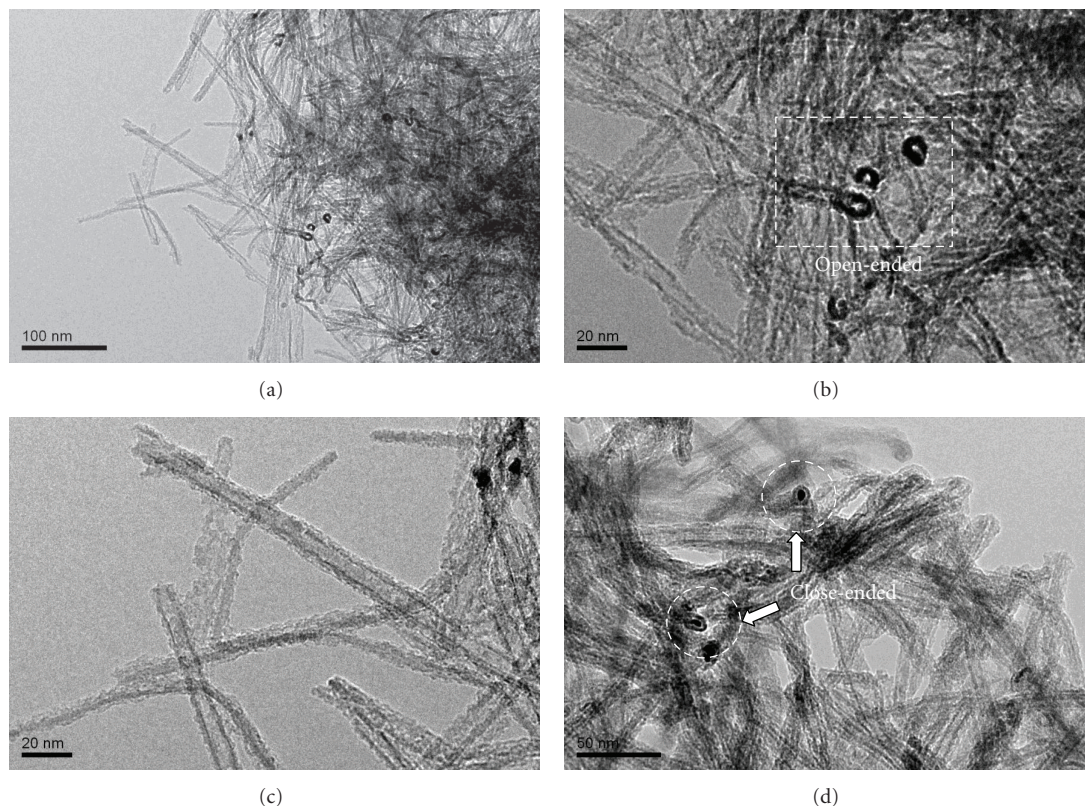


FIGURE 5: TEM images of (a), (b), and (c) $\text{TiO}_2\text{-NTs}@\text{SiO}_2$ with “open-ended” structure (650°C , 2 h). (d) $\text{TiO}_2\text{-NRs}@\text{SiO}_2$ with “close-ended” structure (700°C , 2 h).

reaction time, which is in good agreement with the SEM results.

As described in our previous work, we noted that a second silica layer, which is coated on carbon-treated sample, can significantly delay the combustion rate of carbon in the following calcination process. This delay is also confirmed by the TG analysis. For example, as shown in Figure 3(b), in case of sample of 9 h, it is found that after 600°C the weight loss of sample is almost constant. However, after SiO_2 treatment the weight loss of the sample increases continuously and finally comes to a constant until 700°C . The result strongly suggests that the carbon combustion rate of the silica-coated sample has been effectively decreased, which indicates that the tubular morphology is gas-supported by CO_2 evolution until 700°C .

3.4. S_{BET} of $\text{TiO}_2\text{-NTs}@\text{SiO}_2$. Based on TG data, it can be calculated that the final stage of combustion occurred at about $550\text{--}700^\circ\text{C}$, so the silica-coated samples are calcined at this temperature range and S_{BET} of the samples is measured. As shown in Figure 4, it is clear that at different hydrothermal treatment time, the obtained S_{BET} is different even under the same calcination condition, which indicates that the different amount of carbon in a gas-supported process has obvious effects on the S_{BET} of the nanocomposites. Moreover, even under the same hydrothermal reaction condition, the obtained S_{BET} of samples is different at different calcination

temperature, which strongly suggests that the carbon combustion rate affects the S_{BET} of the nanocomposites too. After all, the results of S_{BET} indicate that the sample prepared at 9 h hydrothermal treatment and 650°C calcination (9 h/ 650°C) exhibits the highest S_{BET} .

Figures 5(a)–5(c) are TEM images of the $\text{TiO}_2\text{-NTs}@\text{SiO}_2$ (9 h/ 650°C), which show fine one-dimensional structure and open-ended tubular morphology. However, 700°C calcination temperature will cause $\text{TiO}_2\text{-NTs}$ lose their tubular morphology and become the “close-ended” structure (Figure 5(d)).

3.5. Photocatalysis of $\text{TiO}_2\text{-NTs}@\text{SiO}_2$. The photocatalytic activity of the $\text{TiO}_2\text{-NTs}@\text{SiO}_2$ nanocomposites, which are prepared at various hydrothermal temperature and calcination temperature, are evaluated by photodecomposition of methanol. As shown in Figure 6, all of the $\text{TiO}_2\text{-NTs}@\text{SiO}_2$ nanocomposites samples show higher photocatalytic activity than P25. The sample especially (9 h/ 650°C) shows the highest photoactivity of all the samples, which is about 5 times higher than that of P-25.

4. Conclusion

In summary, by changing carbon-treated hydrothermal reaction condition and post-heat-treatment temperature, the effects of gas-supported process on tubular morphology,

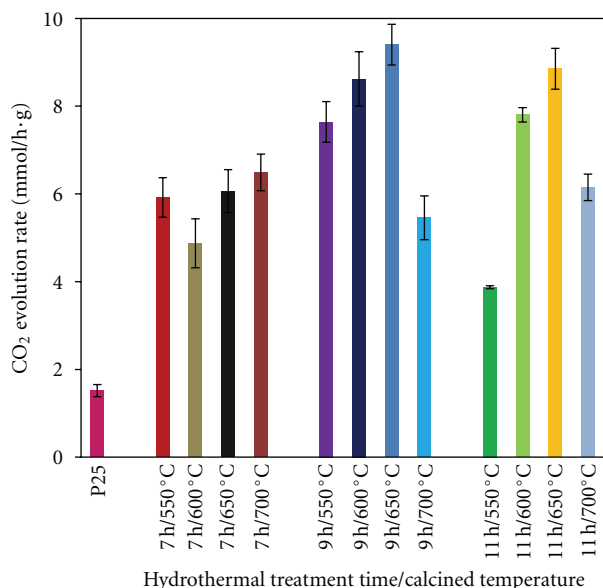


FIGURE 6: Relationship between the amount of CO₂ evolved and photocatalysts with different condition (hydrothermal reaction condition and calcination temperature).

crystallinity and photocatalytic activity of TiO₂-NTs@SiO₂ nanocomposites are investigated. It is found that the sample prepared using hydrothermal treatment (180°C/9 h) and calcination (650°C/2 h) has high-crystallinity and perfect tubular morphology. The sample shows the highest photoactivity of all the samples, which is about 5 times higher than that of P-25.

Acknowledgments

This work was supported by NSFC (50802088, 31070888, 21103152, and 51133006), ZJNSF (R2101054, Y4080392, and Y4100045), Zhejiang Welfare Technology Applied Research Project (2012C23050), and ZJQJSF (2010R10023).

References

- [1] R. Wang, K. Hashimoto, A. Fujishima et al., "Light-induced amphiphilic surfaces," *Nature*, vol. 388, no. 6641, pp. 431–432, 1997.
- [2] G. Palmisano, V. Augugliaro, M. Pagliaro, and L. Palmisano, "Photocatalysis: a promising route for 21st century organic chemistry," *Chemical Communications*, no. 33, pp. 3425–3437, 2007.
- [3] D. Ravelli, D. Dondi, M. Fagnoni, and A. Albini, "Photocatalysis. A multi-faceted concept for green chemistry," *Chemical Society Reviews*, vol. 38, no. 7, pp. 1999–2011, 2009.
- [4] M. N. Chong, B. Jin, C. W. K. Chow, and C. Saint, "Recent developments in photocatalytic water treatment technology: a review," *Water Research*, vol. 44, no. 10, pp. 2997–3027, 2010.
- [5] H. Tong, S. Ouyang, Y. Bi, N. Umezawa, M. Oshikiri, and J. Ye, "Nano-photocatalytic materials: possibilities and challenges," *Advanced Materials*, vol. 24, pp. 229–251, 2012.

- [6] O. Beckstein, P. C. Biggin, and M. S. P. Sansom, "A hydrophobic gating mechanism for nanopores," *Journal of Physical Chemistry B*, vol. 105, no. 51, pp. 12902–12905, 2001.
- [7] J. Lee, H. Kim, S. J. Kahng et al., "Bandgap modulation of carbon nanotubes by encapsulated metallofullerenes," *Nature*, vol. 415, no. 6875, pp. 1005–1008, 2002.
- [8] L. Yang, T. A. Harroun, T. M. Weiss, L. Ding, and H. W. Huang, "Barrel-stave model or toroidal model? A case study on melittin pores," *Biophysical Journal*, vol. 81, no. 3, pp. 1475–1485, 2001.
- [9] J. K. Holt, A. Noy, T. Huser, D. Eaglesham, and O. Bakajin, "Fabrication of a carbon nanotube-embedded silicon nitride membrane for studies of nanometer-scale mass transport," *Nano Letters*, vol. 4, no. 11, pp. 2245–2250, 2004.
- [10] J. Zhang, X. Liu, R. Blume, A. Zhang, R. Schlögl, and D. S. Su, "Surface-modified carbon nanotubes catalyze oxidative dehydrogenation of n-butane," *Science*, vol. 322, pp. 73–77, 2008.
- [11] M. Zhang, Z. Jin, J. Zhang et al., "Effect of annealing temperature on morphology, structure and photocatalytic behavior of nanotubed H₂Ti₂O₄(OH)₂," *Journal of Molecular Catalysis A*, vol. 217, pp. 203–210, 2004.
- [12] G. H. Du, Q. Chen, R. C. Che, Z. Y. Yuan, and L. P. Peng, "Preparation and structure analysis of titanium oxide nanotubes," *Applied Physics Letters*, vol. 79, no. 22, p. 3702, 2001.
- [13] T. Wang, S. Wang, W. Chen et al., "Chemical morphology freezing: chemical protection of the physical morphology of high photoactivity anatase TiO₂ nanotubes," *Journal of Materials Chemistry*, vol. 19, no. 27, pp. 4692–4694, 2009.
- [14] S. Wang, T. Wang, Y. L. Gao, Y. W. Ding, G. H. Jiang, and W. X. Chen, "Wet photochemical filling: a new low-diameter tube-filling method based on differentiated nanotube surfaces," *Journal of Materials Chemistry*, vol. 21, no. 48, pp. 19337–19343, 2011.
- [15] J. F. Banfield, S. A. Welch, H. Zhang, T. T. Ebert, and R. L. Penn, "Aggregation-based crystal growth and microstructure development in natural iron oxyhydroxide biomineralization products," *Science*, vol. 289, no. 5480, pp. 751–754, 2000.

